An Iridium-Pentahydride Referee for Competition of Activations between C-H and C-F Bonds and between C-H Bonds Located in Different Positions

Ana Berges, Miguel A. Esteruelas, Ana M. López, Cristina Martín-Escura, and Enrique Oñate*

Departamento de Química Inorgánica, Instituto de Síntesis Química y Catálisis Homogénea (ISQCH), Centro de Innovación en Química Avanzada (ORFEO-CINQA), Universidad de Zaragoza-CSIC, 50009 Zaragoza, Spain.

ABSTRACT: Polyhydride $IrH_5(P^iPr_3)_2$ (**1**) activates an *ortho*-CH bond of acetophenone and an *ortho*-CF bond of 2,3,4,5,6-pentafluoroacetophenone to give $IrH_2\{\kappa^2\text{-}C,O\text{-}[C_6H_4C(O)CH_3]\}(P^iPr_3)_2$ (**2**) and $IrH_2\{\kappa^2\text{-}C,O\text{-}[C_6F_4C(O)CH_3]\}(P^iPr_3)_2$ (**3**). When the phenyl group contains *ortho*-CH and *ortho*-CF bonds, *ortho*-CH bond activation is kinetically favored. Thus, complexes $IrH_2\{\kappa^2\text{-}C,O\text{-}[C_6H_3FC(O)CH_3]\}(P^iPr_3)_2$ (**4**) and $IrH_2\{\kappa^2\text{-}C,O\text{-}[C_6H_4C(O)C_6H_3F_2]\}(P^iPr_3)_2$ (**5**) are obtained from the reactions of **1** with 2-fluoroacetophenone and 2,6-difluorobenzophenone. Complex **1** also activates an *ortho*-CH bond of the 4-fluorophenyl group of 2-(4-fluorophenyl)pyridine. The reaction leads to $IrH_2\{\kappa^2\text{-}C,N\text{-}[C_6H_3F\text{-}py]\}(P^iPr_3)_2$ (**6**). Replacement of the hydrogen atom of one of the *ortho*-CH bonds with a fluorine accelerates orthometalation, while the *ortho*-CH and *ortho*-CF bonds compete for the metal center. Thus, 2-(2,4-difluorophenyl)pyridine produces a 1:9 mixture of **6** and $IrH_2\{\kappa^2\text{-}C,N\text{-}[C_6H_2F_2\text{-}py]\}(P^iPr_3)_2$

(**7**). Complex **1** activates in a competitive manner *ortho*-CH and *ortho*-CF bonds of 2,6-bis(2,4-difluorophenyl)pyridine to give mixtures of IrH{κ^3-*C,N,C*-[$C_6H_2F_2$-py-$C_6H_2F_2$]}(P^iPr_3)$_2$ (**8**) and IrH{κ^3-*C,N,C′*-[$C_6H_2F_2$-py-C_6H_3F]}(P^iPr_3)$_2$ (**9**). H/D Isotopic exchange experiments indicate that these orthometalations are thermodynamically assisted by chelating effect resulting from coordination of carbonyl or pyridyl groups. However, the activation of other C(sp^2)–H bonds less sterically hindered is kinetically favored. The distribution of deuterium atoms in the orthometalated phenyl ring also shows kinetic preference for the activation of bonds located *ortho* to fluorine.

INTRODUCTION

Because C–H bonds are ubiquitous in organic compounds and often have similar properties to each other, one of the biggest challenges in chemistry today is understanding why and how one of them in particular can be cleaved to promote selective functionalization at that position.[1] In this context, C–H bond activation reactions promoted by transition metals are of great relevance from a fundamental point of view.[2] In addition, they connect with a breadth of fields, ranging from organic[3] and organometallic[4] synthesis to catalysis[5] and materials science.[6]

Halides are versatile functional groups. The enthalpy of the C–halide bond decreases as we move down in group 17 of the periodic table. Thus, the C–F bond is stronger than the rest of the C–halide bonds. As a result, fluorinated organic compounds are gaining importance in several fields of practical application, including medicine, new materials, or the agrochemical industry, among others.[7] The presence of fluorine modifies the properties of fluorinated compounds compared to non-fluorinated ones, particularly medicinal[8] and agrochemical agents,[9] reducing their negative side effects.[10] The relevance of this class of molecules makes their

postfunctionalization an objective of great fundamental and practical interest.[11] In principle, the functionalization process can be carried out in C–H or C–F positions when both bonds are present in the molecule. It involves the selective cleavage of a C–H bond, in the former, while the selective cleavage of a C–F bond is the key step of postfunctionalization, in the latter. From this perspective, the selectivity in the competition between the activation of C–H and C–F bonds emerges as an issue to be resolved, which must be added to the problem of selectivity in the competition between the activation of the different C–H bonds. The addition of a C–F bond to an unsaturated metal center, of a transition metal complex, in the presence of C–H bonds is thermodynamically possible. Although generally the C–F bond is stronger than the C–H bond regardless of carbon hybridization, M–F bonds are notably stronger than M–H bonds for any transition metal.[12] The difference in most cases is enough to master the balance. Despite it, C–H bond activation is observed more frequently than C–F bond activation in fluoroarenes, with late transition metal complexes, particularly for 4d and 5d metals. This suggests that kinetic factors dominate the competition between activations, for these substrates.[13]

The position of the fluorine substituent in fluoroarenes dramatically influences the competition between the different C–H bonds for activation. The strength of both C–H and M–C bonds increases with the number of *ortho*-fluorine substituents, but the latter does so more strongly. The result is a thermodynamic preference for the formation of the M–C bond with more *ortho*-fluorine groups. The impact on the *meta* and *para* positions is much smaller.[11f,13] The thermodynamic *ortho-fluorine effect* was already demonstrated experimentally in the pioneering work of Jones and Perutz on the activation of a C–H bond of 1,3-difluorobenzene, promoted by Rh(η^5-C_5Me_5)(PMe_3), by observing that the 5:1 kinetic mixture of the isomers RhH(2,4-$F_2C_6H_3$)(η^5-C_5Me_5)(PMe_3) and RhH(3,5-$F_2C_6H_3$)(η^5-C_5Me_5)(PMe_3) was transformed into the thermodynamic product RhH(2,6-

$F_2C_6H_3(\eta^5\text{-}C_5Me_5)(PMe_3)$, after 20 h, at 78 ºC.[14] The composition of the initial mixture is consistent with a kinetic preference for the activation of a C–H bond *ortho* to only a C–F bond. Accordingly, the preferential formation of the $R_3Si(2,4\text{-}F_2C_6H_3)$ isomer has been observed for the iridium-catalyzed silylation of 1,3-difluorobenzene; a process that is kinetically controlled by the activation energy of the C–H cleavage of the bond to be silylated.[15]

The presence of a coordinating function in the aromatic compound provides thermodynamic selectivity for the activation of one of the positions *ortho* to said group. The coordination of said function stabilizes the activation product by chelate effect, regardless of the C–H or C–F nature of the cleaved bond and the positions of the fluoride substituents. When the substitution is asymmetric with respect to the coordinating function, the *ortho* bond that wins the competition depends on different factors, including the metal center, the ligands of the complex, and the byproducts of activation. In this case, the kinetics of the bond rupture process can play a relevant role. Cyclometalations of this type have been described mainly for metals of groups 8,[16-18] 9,[19-21] and 10.[22-24]

Polyhydride complexes of platinum group metals have proven to be particularly useful tools for promoting σ bond activations;[25] a property, which has given them special relevance in catalysis[26] and as synthetic precursors in the development of challenging procedures to prepare novel phosphorescent emitters.[6d] One of the most prominent complexes of this type with such qualities is the iridium pentahydride $IrH_5(P^iPr_3)_2$ (**1**).[27] This polyhydride is currently prepared in high yield (>75%) from the iridium(III) complex $IrHCl_2(P^iPr_3)_2$, by treatment with $NaBH_4$.[27g] The reaction initially leads to the tetrahydroborate $IrH_2\{\kappa^2\text{-}H,H\text{-}[BH_4]\}(P^iPr_3)_2$, which decomposes at room temperature, dissolved in alcohols, to produce the pentahydride.[28] The ability of **1** to activate σ bonds prompted us to experimentally study the selectivity in the competition between the

activation of C–H and C–F bonds and between the activation of different C–H bonds, in fluorinated acetophenones and phenyl-fluorinated 2-phenyl-pyridines, with this polyhydride. This article shows the thermodynamic and kinetic preferences in each competition.

RESULTS AND DISCUSSION

Reactions of 1 with Fluorinated Acetophenones. This pentahydride activates *ortho*-CH and *ortho*-CF bonds of acetophenone-type molecules (Scheme 1). Treatment of the polyhydride with 1.0 equiv of acetophenone, in toluene, at reflux, for 4 h quantitatively leads to the dihydride $IrH_2\{\kappa^2\text{-}C,O\text{-}[C_6H_4C(O)CH_3]\}(P^iPr_3)_2$ (**2**), as a result of the release of two hydrogen molecules and the cyclometalation of the ketone. Under the same conditions, 2,3,4,5,6-pentafluoroacetophenone produces the tetrafluorinated derivative $IrH_2\{\kappa^2\text{-}C,O\text{-}[C_6F_4\text{-}C(O)CH_3]\}(P^iPr_3)_2$ (**3**), although the reaction is dirtier than for acetophenone, with some decomposition of the starting polyhydride and some secondary products observed. The formation of **3** is a consequence of the release of one molecule of hydrogen and another of hydrogenfluoride, in addition to the cleavage of the *ortho*-CF bond of the ketone. The removal of hydrogen fluoride is consistent with the greater strength of the H–F bond compared to the H–H bond.

Scheme 1. Reactions of 1 with Acetophenone and 2,3,4,5,6-Pentafluoroacetophenone

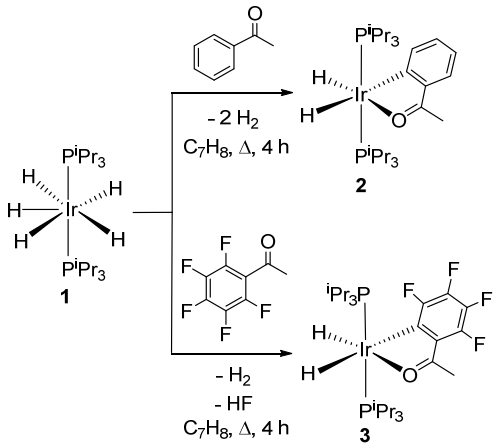

Complexes **2** and **3** were isolated as orange solids in only moderate yields (20–40%), due to their high solubility in non-polar solvents and moderate solubility in methanol. Complex **3** was characterized by X-ray diffraction analysis (Figure 1). The structure confirms the activation of the *ortho*-C–F bond. The polyhedron around the iridium center is the usual octahedron for a six-coordinate d^6-ion, with the phosphine ligands *trans*-arranged (P(1)–Ir–P(2) = 159.439(18)º), while the chelate group and the hydrides lie in a plane perpendicular to the P–Ir–P direction. The NMR spectra of the obtained solids are consistent with this ligand distribution. Thus, the ^{1}H spectra contain two triplets of doublets in the high field region, due to the inequivalent hydrides, whereas the $^{31}P\{^{1}H\}$ spectra show a singlet corresponding to the equivalent phosphines (Table 1).

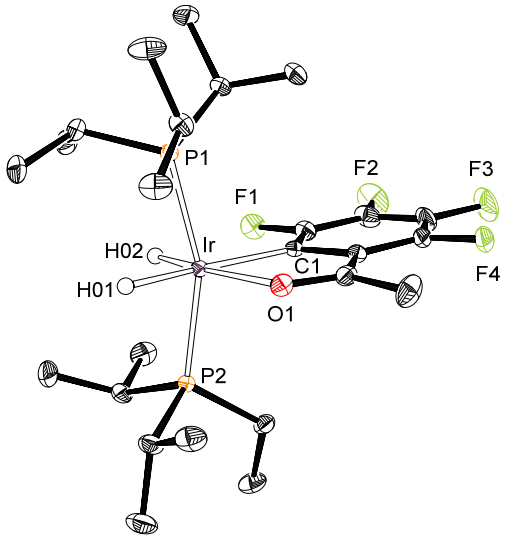

Figure 1. Molecular structure of **3** (50% probability ellipsoids; hydrogen atoms, except hydride ligands, have been omitted). Selected bond lengths (Å) and angles (deg): Ir-C(1) = 2.0739(19), Ir-O(1) = 2.2189(14), Ir-H(01) = 1.65(2), Ir-H(02) = 1.52(2), Ir-P(1) = 2.2988(5), Ir-P(2) = 2.2971(5); P(1)-Ir-P(2) = 159.439(18)º, C(1)-Ir-H(01) = 174.5(8), O(1)-Ir-H(02) = 171.9(9), C(1)-Ir-O(1) = 76.01(7).

Table 1. Selected Resonance Signals of Complexes 2–9 in Their ^{1}H, $^{31}P\{^{1}H\}$, and $^{13}C\{^{1}H\}$, NMR Spectra in C_6D_6 at 298 K[a]

Complex	^{1}H				$^{31}P\{^{1}H\}$		$^{13}C\{^{1}H\}$	
	δ Ir-H	$^{2}J_{HP}$	$^{2}J_{HH}$	Figure	δ Ir-P	Figure	δ Ir-C	Figure
2	-11.66 -27.17	20.9 16.8	5.4	S4	34.5	S5	198.5	S6
3	-12.17 -27.16	20.5 16.5	6.4	S7, S8	35.4	S9	176.0	S12
4	-11.69 -27.01	20.9 16.7	5.4	S14, S15	34.4	S16	203.6	S19
5	-11.28 -27.18	21.2 16.6	5.5	S21, S22	38.0	S23	205.5	S26
6	-12.65 -20.87	21.0 18.6	4.7	S28, S29	26.2	S30	182.3	S33
7	-12.85 -20.85	19.5 18.6	4.7	S35, S36	26.2	S37	185.7	S40
8	-15.52	19.8		S41	2.9	S42	171.5	S45
9	-15.47	19.8		S46	4.5	S47	172.5 168.3	S50

[a] δ in ppm and *J* in Herzt.

The activation of the *ortho*-CH bond of the phenyl group of the ketone is clearly favored from a thermodynamic point of view, with respect to the activation of the C–H bonds in the rest of the positions, due to the chelating effect provided by the coordination of the oxygen atom. However, it is also evident that the acyl group exerts an important steric obstacle on the *ortho*-CH bonds, which kinetically should disfavor their activation. To confirm this, we carried out the reaction of the pentadeuteride $IrD_5(P^iPr_3)_2$ (**1*d*$_5$**) with acetophenone. Under the same conditions as those mentioned for the formation of **2**, using toluene-d_8 as a solvent instead of toluene, the reaction leads to the trideuterated species $IrH_2\{\kappa^2\text{-}C,O\text{-}[C_6D_3HC(O)CH_3]\}(P^iPr_3)_2$ (**2*d*$_3$** in Scheme 2), as a result of the release of one molecule of deuterium and another of hydrogen, the C–H bond

activation of the phenyl group of the ketone, and H/D isotopic exchanges between the latter and the pentadeuteride precursor.

Scheme 2. Reaction of 1*d*$_5$ with Acetophenone[a]

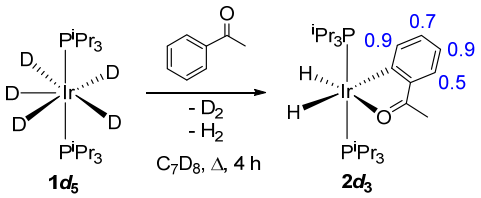

[a]Values in blue denote the extent of deuteration.

The reaction yields three findings of special relevance: the distribution of deuterium within the phenyl group, which decreases in the sequence with respect to the acyl group: *meta* (*ortho* to IrC; 0.9) = *meta* (*para* to IrC, 0.9) > *para* (0.7) > *ortho* (0.5); the total protiation of the metallic center; and the transfer of exactly three deuterides from the iridium atom to the activated phenyl group. The lower deuteration of the *ortho* position is consistent with a C–H bond activation process kinetically controlled by steric factors; activation of C–H bonds at the *meta* and *para* positions is kinetically preferred to that at the *ortho* positions, but once an *ortho*–CH bond is activated, the activation product is stabilized by oxygen coordination. In other words, the activation of the *ortho*-CH bond of the phenyl group is a chelate-assisted process.[17b,27d,29] The presence of two protiums in the metal center and three deuteriums in the activated phenyl group means that: (i) the metal species responsible for the activation of the C–H bond is the unsaturated trideuteride $IrD_3(P^iPr_3)_2$, which is generated by reductive elimination of the molecular deuterium from **1*d*$_5$**, and (ii) any C–D reductive elimination in the iridium(V) intermediate resulting from C–H addition is faster than H–D reductive elimination. On this basis, the formation of **2** can be rationalized through the events summarized in Scheme 3. The dissociation of the molecular hydrogen from **1** generates the trihydride intermediate $IrH_3(P^iPr_3)_2$, which adds the *ortho*-CH bond of the phenyl substituent of

the ketone to produce an iridium(V) intermediate. Reductive elimination of molecular hydrogen from the latter followed by coordination of the oxygen atom of the acyl group gives the isolated product. The formation of **3** most likely follows a similar pathway, involving the addition of C–F to $IrH_3(P^iPr_3)_2$ and the reductive removal of hydrogen fluoride from the resulting iridium(V) intermediate.

Scheme 3. Proposed Pathway for the Formation of Complex 2

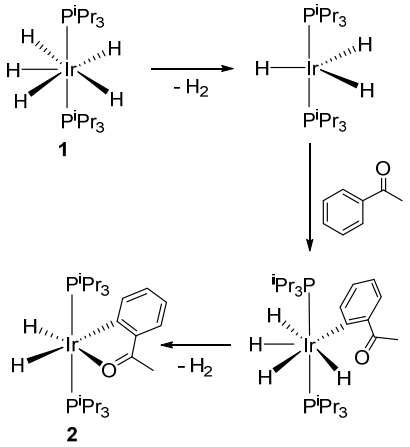

Having established that complex **1** activates the *ortho*-CH and *ortho*-CF bonds of acetophenone-type substrates, we decided to investigate what happens when both bonds are on the same phenyl group. Thus, we decided to investigate the reactions with 2-fluoroacetophenone. Treatment of **1** with 1.0 equiv of this ketone under the aforementioned conditions selectively and quantitatively leads to $IrH_2\{\kappa^2\text{-}C,O\text{-}[C_6H_3FC(O)CH_3]\}(P^iPr_3)_2$ (**4**), as a result of the activation of the *ortho*-CH bond, in the presence of the *ortho*-CF bond. The reaction of **1*d*$_5$** with the ketone indicates that, as in the previous case, the activation is a chelate-assisted process as demonstrated by the deuteration of the rest of the positions of the aromatic ring in the partially deuterated obtained dihydride $IrH_2\{\kappa^2\text{-}C,O\text{-}[C_6D_{2.5}H_{0.5}FC(O)CH_3]\}(P^iPr_3)_2$ (**4*d*$_{2.5}$**). Furthermore, the distribution of deuterium in the orthometalated phenyl group is consistent with the *ortho-fluorine*

effect; of the two *meta* positions with respect to the acyl group, the one located *ortho* to the fluoride substituent is deuterated twice as much as the one located in the *para* position (Scheme 4).

Scheme 4. Reactions of 1 and 1d_5 with 2-Fluoroacetophenone[a]

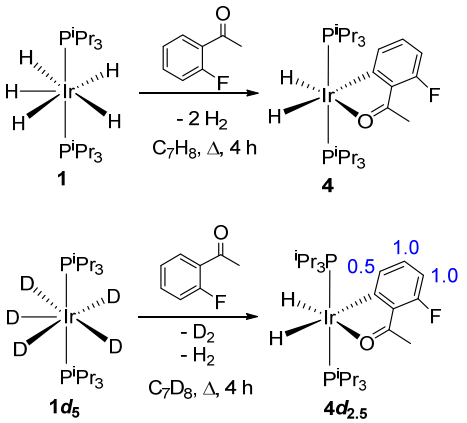

[a]Values in blue denote the extent of deuteration.

Complex **4** was isolated as an orange solid, in approximately 50% yield, and characterized by X-ray diffraction analysis. The structure (Figure 2) resembles that of **3** and confirms the selective activation of the *ortho*-CH bond. The NMR spectra of the solid obtained are consistent with the structure and agree well with those of **2** and **3** (Table 1).

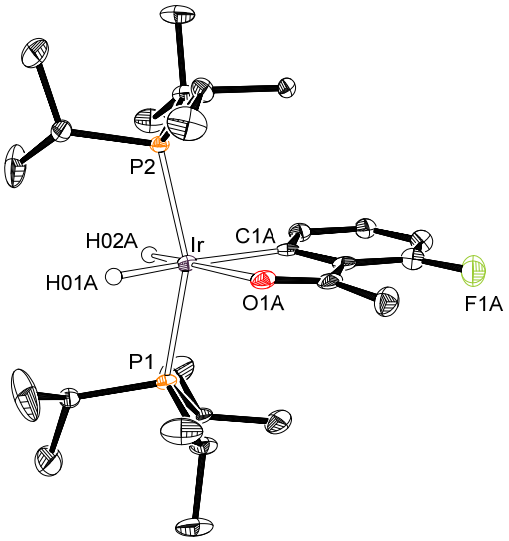

Figure 2. Molecular structure of **4** (50% probability ellipsoids; hydrogen atoms, except hydride ligands, have been omitted). Selected bond lengths (Å) and angles (deg): Ir-C(1A) = 2.120(4), Ir-O(1A) = 2.226(7), Ir-P(1) = 2.302(2), Ir-P(2) = 2.296(2); P(1)-Ir-P(2) = 157.10(7), C(1A)-Ir-H(01A) = 175.7(8), O(1A)-Ir-H(02) = 167.8(7), C(1A)-Ir-O(1A) = 76.0(3).

The osmium-hexahydride complex $OsH_6(P^iPr_3)_2$ also activates the *ortho*-CH and *ortho*-CF bonds of aromatic ketones. For competitive processes, it shows selectivity toward C–H bond activation when the *ortho*-CH and *ortho*-CF bonds are on the same phenyl group. However, the *ortho*-CF bond is selectively activated in molecules containing two different phenyl groups, one of them with two *ortho*-CH bonds and the other with two *ortho*-CF bonds.[18a] In contrast, stannyl-osmium(IV)-trihydride $OsH_3(SnPh_2Cl)(P^iPr_3)_2\{\eta^2\text{-}C,C;\kappa^1\text{-}P\text{-}[CH_2{=}C(CH_3)P^iPr_2]\}(P^iPr_3)$[18b] and tetrahydride $OsH_4\{\kappa^3\text{-}P,O,P\text{-}[xant(P^iPr_2)_2]\}$[17b] selectively activate an *ortho*-CH bond of both types of ketones. Pentahydride **1** shows a behavior similar to that of the latter two (Scheme 5). Thus, its reaction with 2,6-difluorobenzophenone produces $IrH_2\{\kappa^2\text{-}C,O\text{-}[C_6H_4C(O)C_6H_3F_2]\}(P^iPr_3)_2$ (**5**). According to the $^{31}P\{^1H\}$ NMR spectrum of the reaction crude, complex **5** is a result of the selective and quantitative activation of one of the *ortho*-CH bonds of the non-fluorinated phenyl group. It was isolated as an orange solid in approximately 60% yield. In this context, it should be mentioned that the increase in steric hindrance around the carbonyl group has a significant influence on the rate of formation of the dihydride product. The reaction of **1** with 2,6-difluorobenzophenone is significantly slower than the reaction with acetophenone. The replacement of the methyl group by the 2,6-difluorophenyl unit produces an increase in the reaction time necessary for the quantitative formation of the dihydride product; complex **5** was obtained after 9 h of reaction, 5 h more than the time necessary to form **2**. This slowdown can be attributed to a decrease in the coordination ability of the oxygen atom. This influences the

deuterium content of the reaction product of the pentadeuteride **1*d*$_5$** with 2,6-difluorobenzophenone, in toluene-d_8, revealing H/D isotopic exchanges between the ketone and the reaction solvent through the metal center. Thus, unlike the previous cases, it contains more than three deuterium atoms, as a result of a competitive activation process between the C–H bonds of the ketone and the solvent; around 0.5 in each hydride position, 3.5 in the orthometalated phenyl group and approximately 3 in the fluorinated phenyl ring. The almost complete deuteration of the fluorinated ring in **4** and **5** is consistent with a kinetic preference for the activation of the C–H bonds over the activation of the C–F bonds, in accordance with the general trend in this type of reactions.

Scheme 5. Reactions of 1 and 1*d*$_5$ with 2,6-Difluorobenzophenone[a]

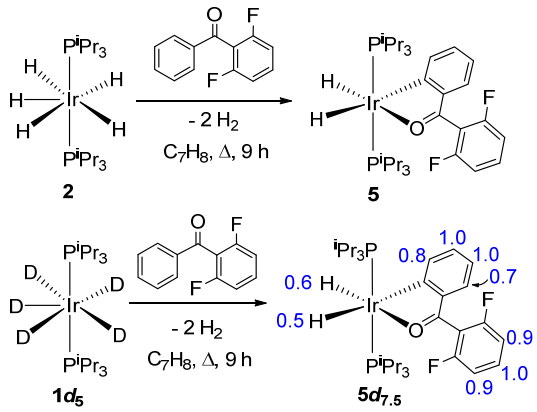

[a]Values in blue denote the extent of deuteration.

Reactions of 1 with Fluorinated 2-Phenylpyridines. Complex **1** also activates an *ortho*-CH bond of 2-(4-fluorophenyl)pyridine to give a dihydride derivative related to those obtained with the above aromatic ketones, although the reaction is significantly slower (Scheme 6). Treatment of the pentahydride with the heterocycle, in toluene, at reflux, for 16 h leads to $IrH_2\{\kappa^2$-*C,N*-$[C_6H_3F$-py$]\}(P^iPr_3)_2$ (**6**), which was isolated as a yellow solid in high yield, 87%. The ^1H and $^{31}P\{^1H\}$ NMR spectra of this solid support the octahedral structure proposed in Scheme 6 for the

compound, in a consistent manner with the ^{1}H and $^{31}P\{^{1}H\}$ spectra of **2**–**5** (Table 1). In agreement with the reaction of **1*d*$_5$** with 2,6-difluorobenzophenone (the slowest of those studied previously), treatment of the pentadeuteride with 2-(4-fluorophenyl)pyridine, in toluene-*d*$_8$, gives rise to H/D isotopic exchanges between the phenylpyridine and toluene-*d*$_8$, through the metal center. Thus, the partially deuterated dihydride product contains more than three deuterium atoms; 0.5 deuterium equally distributed in the hydride positions, 3 deuterium distributed among the four possible positions of the pyridyl group, and 1.5 deuterium distributed among the three positions of the orthometalated phenyl group. The amount in the different positions is a function of the steric hindrance, decreasing as the latter increases, as expected for a C–H activation process thermodynamically assisted by the chelating effect of the pyridyl group in the *ortho* position, but kinetically controlled by the steric hindrance on the position that is activated. The distribution of deuterium in the orthometalated phenyl ring is as well consistent with the *ortho-fluorine effect*, although positions *ortho* to the fluoride substituent are additionally *meta* with respect to the pydidyl group and thus those that have fewer steric impediments for being activated. The formation of **6** should involve the same events as the formation of **2**–**5**, according to Scheme 3.

Scheme 6. Reactions of 1 and 1*d*$_5$ with 2-(4-Fluorophenyl)pyridine[a]

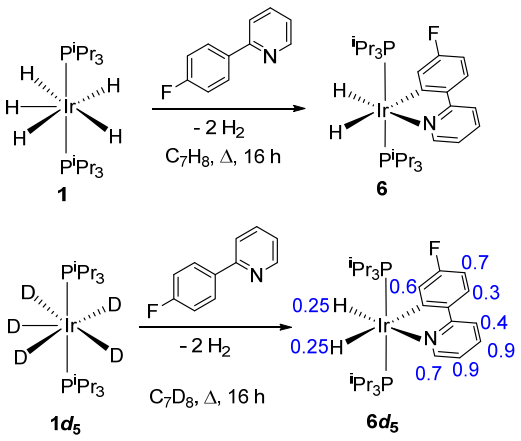

[a]Values in blue denote the extent of deuteration.

Substitution of the hydrogen atom of one of the *ortho*-CH bonds of the 4-fluorophenyl substituent of pyridine with a fluorine accelerates orthometalation, although the *ortho*-CH and *ortho*-CF bonds of the phenyl group compete for the metal center of the unsaturated trihydride intermediate. Thus, the reaction of **1** with 2-(2,4-difluorophenyl)pyridine in toluene, at reflux, produces a mixture of **6** and $IrH_2\{\kappa^2$-*C,N*-$[C_6H_2F_2$-py$]\}(P^iPr_3)_2$ (**7**). Complex **6** results from *ortho*-CF cleavage, while dihydride **7** is generated from the *ortho*-CH bond activation (Scheme 7). The mixture reaches a molar ratio between **6** and **7** of 1:9, when complex **1** completely disappears after only 4 h. An increase in temperature, 186 ºC, in decalin again produces an acceleration of the reaction, as expected, but the solid obtained after cooling the solution does not show a significant change in its composition. This suggests thermodynamic control of the mixture composition. Complexes **6** and **7** co-crystallized from benzene at 4 ºC to produce crystals suitable for X-ray diffraction analysis. Figure S1 shows the structures of both, which confirm the octahedral distribution of donor atoms around the iridium center. The ^1H, $^1H\{^{19}F\}$, $^{31}P\{^1H\}$, $^{19}F\{^1H\}$, and $^{13}C\{^1H\}$ NMR spectra of the mixture (Figures S35-S40) are consistent with the structures.

Scheme 7. Reaction of 1 with 2-(2,4-Difluorophenyl)pyridine

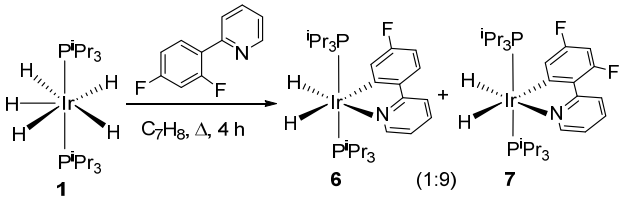

Pincer ligands have gained great importance in chemistry in the last two decades.[30] In this context, osmium-hexahydride $OsH_6(P^iPr_3)_2$[31] and iridium-pentahydride **1**[27c] activate an *ortho*-CH bond of each phenyl substituent of 2,6-diphenylpyridine to produce hydride derivatives stabilized by a *C,N,C*-pincer ligand. These activations inspired us to study the competition between *ortho*-

CH and *ortho*-CF activations in 2,6-bis(2,4-difluorophenyl)pyridine and compare the behavior of this pro-pincer pyridine with the previous pro-chelate pyridines. Complex **1** activates the *ortho*-CH and *ortho*-CF bonds of this fluorinated 2,6-diphenylpyridine. The reaction leads to mixtures of the monohydride-iridium(III)-(*C,N,C*-pincer) derivatives IrH{κ^3-*C,N,C*-[$C_6H_2F_2$-py-$C_6H_2F_2$]}(P^iPr_3)$_2$ (**8**) and IrH{κ^3-*C,N,C´*-[$C_6H_2F_2$-py-C_6H_3F]}(P^iPr_3)$_2$ (**9**). The first results from the activation of the *ortho*-CH bond of both substituents, while the second is generated as consequence of the activation of the *ortho*-CH bond of one substituent and the *ortho*-CF bond of the other. Unlike the reaction of **1** with 2-(2,4-difluorophenyl)pyridine, the composition of the mixture depends on the reaction conditions (Scheme 8). In toluene, at reflux, the solid obtained after 40 hours has a molar ratio between **8** and **9** of approximately 2:1. However, when working in decalin at 186 °C, after 4 h a solid was formed containing 10% of **8** and 90% of **9**. This indicates that the activation of the *ortho*-CH bond of both substituents is kinetically favored, while from a thermodynamic point of view the activation of the *ortho*-CF bond of at least one of the substituents is preferred. Complexes **8** and **9** were inseparable by column or preparative thin layer chromatography on silica gel. Like **6** and **7**, they co-crystallized from benzene at 4 °C to afford crystals suitable for X-ray diffraction analysis. Figures S2 and S3 give views of the connectivity between atoms. The most notable features of these compounds in the ^1H and $^{31}P\{^1H\}$ NMR spectra (Table 1) are a triplet in the high-field region of the former, due to the hydride ligand, and a singlet in the latter. The NMR spectra of $^{13}C\{^1H\}$ and $^{19}F\{^1H\}$ (Figures S43-S45 and S48-S50) are consistent with the octahedral structures shown in Figures S2 and S3.

Scheme 8. Reaction of 1 with 2,6-Bis(2,4-difluorophenyl)pyridine

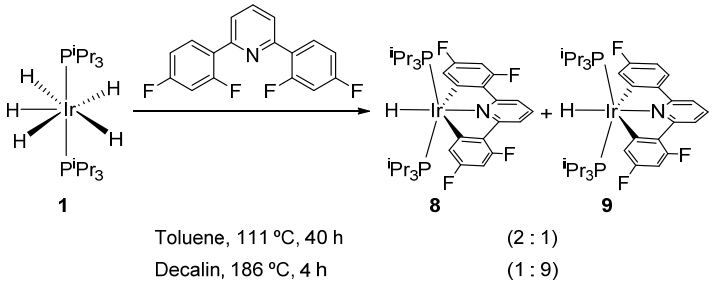

CONCLUDING REMARKS

Pentahydride $IrH_5(P^iPr_3)_2$ activates *ortho*-CH and *ortho*-CF bonds of fluorinated acetophenones and fluorinated 2-phenylpyridines, to form $IrH_2\{\kappa^2\text{-}C,X\text{-}L\}(P^iPr_3)_2$ (X = O, N) or $IrH\{\kappa^3\text{-}C,N,C\text{-}L\}(P^iPr_3)_2$ complexes. H/D Isotopic exchange experiments indicate that the activation of an *ortho*-CH bond of the phenyl group of these molecules is thermodynamically assisted by the chelating effect resulting from the coordination of the carbonyl or pyridyl groups. However, the activation of the $C(sp^2)$–H bonds less sterically hindered is kinetically favored. The distribution of deuterium atoms in the orthometalated phenyl ring also indicates kinetic preference for the activation of C–H bonds located in the *ortho* position with respect to the fluorine substituent. In pro-ligands where the phenyl group contains *ortho*-CH and *ortho*-CF bonds, activation of the *ortho*-CH bond is kinetically favored.

EXPERIMENTAL SECTION

All the reactions were performed in dried solvents under argon atmosphere using glove-box and Schlenck techniques. Their course as a function of time was followed by $^{31}P\{^1H]$, ^1H and ^{19}F NMR spectroscopy. Instrumental details and X-ray information are given in the Supporting Information.

Complex **1**[27g] and **1*d*$_5$**[27d] was prepared as reported in the literature. Chemical shifts are expressed in ppm and coupling constants, *J* and *N* ($N = {}^3J_{H\text{-}P} + {}^5J_{H\text{-}P'}$ for ^{1}H or $^1J_{C\text{-}P} + {}^3J_{C\text{-}P'}$ for ^{13}C), in Hertz.

Reaction of Complex 1 with Acetophenone: Preparation of IrH$_2${κ^2-*C*,*O*-[C$_6$H$_4$C(O)CH$_3$]}(P^{i}Pr$_3$)$_2$ (2). A colorless solution of **1** (100 mg, 0.193 mmol) in 5 mL of toluene was treated with acetophenone (22.6 μL, 0.193 mmol) and heated under reflux. After 4 h, the solvent was removed under vacuum and methanol was added to afford an orange solid, which was washed with methanol at -78 °C and vacuum-dried. Yield: 40 mg (33%). Anal. Calcd for $C_{26}H_{51}IrOP_2$: C 49.27; H 8.11. Found: C 48.93; H 7.85. HRMS (electrospray, *m*/*z*): Calcd for $C_{26}H_{50}IrOP_2$ [M - H]$^+$: 633.2962; found: 633.2936. IR (cm^{-1}): ν (IrH) 2266 (w), 1941 (m); ν (CO) 1565 (m). ^{1}H NMR (300 MHz, C_6D_6, 298 K): δ 8.47 (br d, $^3J_{H\text{-}H}$ = 7.4, 1H, H^5), 7.64 (br d, $^3J_{H\text{-}H}$ = 7.9 , 1H, H^2), 7.08 (ddd, $^3J_{H\text{-}H} = {}^3J_{H\text{-}H'}$ = 7.4, $^4J_{H\text{-}H}$ = 1.4, 1H, H^4), 6.89 (ddd, $^3J_{H\text{-}H}$ = 7.9, $^3J_{H\text{-}H}$ = 7.4, $^4J_{H\text{-}H}$ = 1.3, 1H, H^3), 2.39 (t, $^5J_{H\text{-}P}$ = 1.3, 3H, CH$_3$CO), 1.98 (m, 6H, PCH), 1.10 (dvt, *N* = 13.1, $^3J_{H\text{-}H}$ = 7.2, 18H, PCHC*H*$_3$), 1.07 (dvt, *N* = 13.2, $^3J_{H\text{-}H}$ = 7.2, 18H, PCHC*H*$_3$), −11.66 (tdd, $^2J_{H\text{-}P}$ = 20.9, $^2J_{H\text{-}H}$ = 5.4, $^4J_{H\text{-}H}$ = 1.5, 1H, IrH^B), −27.17 (td, $^2J_{H\text{-}P}$ =16.8, $^2J_{H\text{-}H}$ = 5.4, 1H, IrH^A). ^{31}P{^{1}H} NMR (121.5 MHz, C_6D_6, 298 K): δ 34.5 (s). ^{13}C{^{1}H} NMR (75.5 MHz, C_6D_6, 298 K): δ 212.2 (s, CO), 198.5 (t, $^2J_{C\text{-}P}$ = 6.6, IrC^6), 147.2 (s, C^1), 145.4 (s, C^5), 132.1 (s, C^2), 131.1 (s, C^4), 118.8 (s, C^3), 27.5 (vt, *N* = 27.7, PCH), 24.6 (s, CH$_3$CO), 20.1, 20.0 (both s, PCH*C*H$_3$).

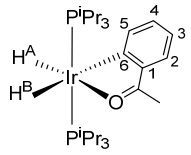

Reaction of Complex 1 with 2,3,4,5,6-Pentafluoroacetophenone: Preparation of IrH$_2${κ^2-*C*,*O*-[C$_6$F$_4$C(O)CH$_3$]}(P^{i}Pr$_3$)$_2$ (3). A colorless solution of **1** (300 mg, 0.579 mmol) in 10 mL of toluene was treated with 2,3,4,5,6-pentafluoroacetophenone (82.4 μL, 0.579 mmol) and heated under

reflux. After 4 h, the solvent was removed under vacuum and methanol was added to afford an orange solid, which was washed with methanol at -78 °C and vacuum-dried. Yield: 80 mg (20%). Anal. Calcd for $C_{26}H_{47}F_4IrOP_2$: C 44.24; H 6.71. Found: C 43.98; H 6.61. HRMS (electrospray, *m*/*z*): Calcd for $C_{26}H_{46}F_4IrOP_2$ [M - H]$^+$: 705.2585; found: 705.2574. IR (cm^{-1}): ν (IrH) 2298 (w), 1995 (w); ν (CO) 1628 (m). ^{1}H NMR (300 MHz, C_6D_6, 298 K): δ 2.52 (dt, $^5J_{H-F}$ = 5.7, $^5J_{H-P}$ = 1.5, 3H, CH_3CO), 1.84 (m, 6H, PCH), 0.97 (dvt, *N* = 20.3, $^3J_{H-H}$ = 6.8, 36H, PCH*CH*$_3$), -12.17 (m, 1H, IrH^B), -27.16 (m, 1H, IrH^A). ^{1}H{^{19}F} NMR (300 MHz, C_6D_6, 298 K): δ 2.52 (t, $^5J_{H-P}$ = 1.5, 3H, CH_3CO), 1.85 (m, 6H, PCH), 0.97 (dvt, *N* = 20.3, $^3J_{H-H}$ = 6.8, 36H, PCH*CH*$_3$), −12.17 (td, $^2J_{H-P}$ = 20.5, $^2J_{H-H}$ = 6.4, 1H, IrH^B), −27.16 (td, $^2J_{H-P}$ = 16.5, $^2J_{H-H}$ = 6.4, 1H, IrH^A). ^{31}P{^{1}H} NMR (121.5 MHz, C_6D_6, 298 K): δ 35.4 (s). ^{19}F NMR (282,33 MHz, C_6D_6, 298 K): δ −105.6 (m, 1F), −134.8 (m, 1F), −149.7 (m, 1F), −166.6 (m, 1F). ^{19}F {^{1}H} NMR (282,33 MHz, C_6D_6, 298 K): δ −105.6 (dd, $^3J_{F-F}$ = 35.6, $^4J_{F-F}$ = 20.8, 1F, F^2 o F^5), −134.8 (ddd, $^3J_{F-F}$ = 22.1, $^3J_{F-F}$ = 20.7, $^4J_{F-F}$ = 6.3, 1F, F^3 o F^4), −149.7 (ddd, $^3J_{F-F}$ = 35.6, $^4J_{F-F}$ = 20.5, $^5J_{F-F}$ = 6.3, 1F, F^2 o F^5), −166.6 (dd, $^3J_{F-F}$ = 21.3, 1F, F^3 o F^4). ^{13}C{^{1}H} NMR (75.5 MHz, C_6D_6, 298 K): δ 207.7 (m, CO), 176.0 (dm, $^2J_{C-F}$ = 62.2, IrC^6), 152.0 (dm, $^1J_{C-F}$ = 263.9, CF), 150.1 (dm, $^1J_{C-F}$ = 221.7, CF), 143.6 (dm, $^1J_{C-F}$ = 268.4, CF), 133.8 (dm, $^1J_{C-F}$ = 240.0, CF), 129.2 (dm, $^2J_{C-F}$ = 19.0, C^1), 29.4 (d, $^4J_{C-F}$ = 9.3, CH_3CO), 27.5 (dvt, *N* = 28.2, PCH), 20.0, 19.7 (both s, PCH*C*H$_3$).

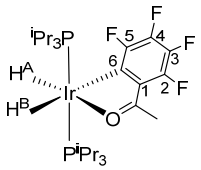

Reaction of Complex 1 with 2-Fluoroacetophenone: Preparation of IrH$_2${κ^2-*C*,*O*-[C$_6$H$_3$FC(O)CH$_3$]}(P^{i}Pr$_3$)$_2$ (4). A colorless solution of **1** (100 mg, 0.193 mmol) in 5 mL of toluene was treated with 2-fluoroacetophenone (28 μL, 0.193 mmol) and heated under reflux. After 4 h,

the solvent was removed under vacuum and methanol was added to afford an orange solid, which was washed with methanol at -78 °C and vacuum-dried. Yield: 60 mg (48%). Anal. Calcd for $C_{26}H_{50}FIrOP_2$: C 47.91; H 7.73. Found: C 47.55; H 7.60. HRMS (electrospray, *m*/*z*): Calcd for $C_{26}H_{49}FIrOP_2$ $[M - H]^+$: 651.2867; found: 651.2844. IR (cm^{-1}): ν (IrH) 2228 (w), 1980 (w), ν (CO) 1598 (w). ^1H NMR (300 MHz, C_6D_6, 298 K): δ 8.15 (br d, $^3J_{H-H}$ = 7.3, 1H, H^5), 6.88 (ddd, $^3J_{H-H}$ = $^3J_{H-H'}$ = 7.6, $^4J_{H-F}$ = 5.2, 1H, H^4), 6.51 (dd, $^3J_{H-F}$ = 12.4, $^3J_{H-H}$ = 7.6, 1H, H^3), 2.77 (dt, $^5J_{H-F}$ = 5.5, $^5J_{H-P}$ = 1.3, 3H, CH_3CO), 1.94 (m, 6H, PCH), 1.07 (dvt, *N* = 13.0, $^3J_{H-H}$ = 5.1, 18H, PCHC*H*$_3$), 1.04 (dvt, *N* = 13.0, $^3J_{H-H}$ = 5.1, 18H, PCHC*H*$_3$), -11.69 (m, 1H, IrH^B), -27.01 (td, $^2J_{H-P}$ = 16.6, $^2J_{H-H}$ = 5.5, 1H, IrH^A). $^1H\{^{19}F\}$ NMR (300 MHz, C_6D_6, 298 K): δ 8.15 (br d, $^3J_{H-H}$ = 7.4, 1H, H^5), 6.88 (dd, $^3J_{H-H}$ = $^3J_{H-H'}$ = 7.6, 1H, H^4), 6.51 (br d, $^3J_{H-H}$ = 7.7, 1H, H^3), 2.77 (t, $^5J_{H-P}$ = 1.5, 3H, CH_3CO), 1.95 (m, 6H, PCH), 1.07 (dvt, *N* = 12.8, $^3J_{H-H}$ = 5.0, 18H, PCHC*H*$_3$), 1.04 (dvt, *N* = 13.1, $^3J_{H-H}$ = 5.1, 18H, PCHC*H*$_3$), −11.69 (tdd, $^2J_{H-P}$ = 20.9, $^2J_{H-H}$ = 5.4, $^6J_{H-H}$ = 1.6, 1H, IrH^B), −27.01 (td, $^2J_{H-P}$ = 16.7, $^2J_{H-H}$ = 5.4, 1H, IrH^A). $^{31}P\{^1H\}$ NMR (121.5 MHz, C_6D_6, 298 K): δ 34.4 (s). ^{19}F NMR (282.33 MHz, C_6D_6, 298 K): δ −108.2 (m). $^{19}F\{^1H\}$ NMR (282.33 MHz, C_6D_6, 298 K): δ −108.2 (s). $^{13}C\{^1H\}$ NMR (75.5 MHz, C_6D_6, 298 K): δ 210.0 (dt, $^3J_{C-F}$ = 6.4, $^2J_{C-P}$ = 1.8, CO), 203.6 (dt, $^3J_{C-F}$ = $^2J_{C-P}$ = 6.1, IrC^6), 167.6 (d, $^1J_{C-F}$ = 262.5, C^2), 141.1 (d, $^4J_{C-F}$ = 3.4, C^5), 134.9 (d, $^2J_{C-F}$ = 2.8, C^1), 132.6 (d, $^3J_{C-F}$ = 7.5, C^4), 104.9 (d, $^2J_{C-F}$ = 22.8, C^3), 29.9 (d, $^4J_{C-F}$ = 9.7, CH_3CO), 27.5 (vt, *N* = 27.9, PCH), 20.1, 19.9 (both s, PCH*C*H$_3$).

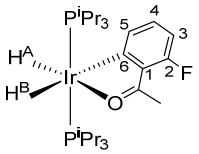

Reaction of Complex 1 with 2,6-Difluorobenzophenone: Preparation of $IrH_2\{\kappa^2$-*C*,*O*-$[C_6H_6C(O)C_6H_3F_2]\}(P^iPr_3)_2$ (5). A colorless solution of **1** (100 mg, 0.193 mmol) in 5 mL of

toluene was treated with 2,6-difluorobenzophenone (33 μL, 0.193 mmol) and heated under reflux. After 9 h, the solvent was removed under vacuum and methanol was added to afford a red solid, which was washed with methanol at -78 °C and vacuum-dried. Yield: 80 mg (56%). Anal. Calcd for $C_{31}H_{51}F_2IrOP_2$: C 50.87; H 7.02. Found: C 50.55; H 6.98. HRMS (electrospray, *m*/*z*): Calcd for $C_{31}H_{52}F_2IrOP_2$ $[M + H]^+$: 733.3087; found: 733.3121. IR (cm^{-1}): ν (IrH) 2272 (w), 1918 (w), ν (CO) 1626 (w). ^{1}H NMR (300 MHz, C_6D_6, 298 K): δ 8.58 (br d, $^3J_{H-H}$ = 7.6, 1H, H^9), 7.66 (br d, $^3J_{H-H}$ = 8.0, 1H, H^6), 7.00 (ddd, $^3J_{H-H}$ = 7.8, $^3J_{H-H'}$ = 6.9, $^4J_{H-H}$ = 1.4, 1H, H^8), 6.80 (ddd, $^3J_{H-H}$ = 8.1, $^3J_{H-H'}$ = 6.9, $^4J_{H-H}$ = 1.2, 1H, H^7), 6.57 (m, 1H, H^4), 6.44 (m, 2H, H^3), 2.09 (m, 6H, PCH), 1.22 (dvt, *N* = 13.7, $^3J_{H-H}$ = 7.0, 18H, PCHCH_3), 1.05 (dvt, *N* = 12.8, $^3J_{H-H}$ = 7.0, 18H, PCHCH_3), -11.27 (tdd, $^2J_{H-P}$ = 21.3, $^2J_{H-H}$ = 5.3, $^6J_{H-H}$ = 1.7, 1H, IrH^B), -2717 (td, $^2J_{H-P}$ = 16.6, $^2J_{H-H}$ = 5.3, 1H, IrH^A). ^{1}H {^{19}F} NMR (300 MHz, C_6D_6, 298 K): δ 8.58 (br d, $^3J_{H-H}$ = 7.6, 1H, H^9), 7.66 (br d, $^3J_{H-H}$ = 7.9 , 1H, H^6), 7.00 (dd, $^3J_{H-H}$ = $^3J_{H-H'}$ = 7.3, 1H, H^8), 6.80 (dd, $^3J_{H-H}$ = $^3J_{H-H'}$ = 7.4, 1H, H^7), 6.58 (dd, $^3J_{H-H}$ = 9.3, $^3J_{H-H'}$ = 7.4, 1H, H^4), 6.45 (d, $^3J_{H-H}$ = 8.3, 2H, H^3), 2.08 (m, 6H, PCH), 1.22 (dvt, *N* = 13.7, $^3J_{H-H}$ = 7.0, 18H, PCHCH_3), 1.05 (dvt, *N* = 13.1, $^3J_{H-H}$ = 6.7, 18H, PCHCH_3), -11.28 (td, $^2J_{H-P}$ = 21.2, $^2J_{H-H}$ = 5.7, 1H, IrH^B), -27.18 (td, $^2J_{H-P}$ = 16.6, $^2J_{H-H}$ = 5.3, 1H, IrH^A). ^{31}P{^{1}H} NMR (121.5 MHz, C_6D_6, 298 K): δ 38.0 (s). ^{19}F NMR (282.33 MHz, C_6D_6, 298 K): δ −110.8 (t, $^3J_{H-F}$ = 6.4, 2F). ^{19}F{^{1}H} NMR (282.33 MHz, C_6D_6, 298 K): δ –110.8 (s). ^{13}C{^{1}H} NMR (75.5 MHz, C_6D_6, 298 K): δ 205.5 (t, $^2J_{C-P}$ = 5.6, IrC^{10}), 200.8 (t, $^3J_{C-P}$ = 2.2, CO), 160.5 (dd, $^1J_{C-F}$ = 250.4, $^3J_{C-F}$ = 7.7, C^2), 147.6 (s, C^5), 146.0 (s, C^9), 134.7 (s, C^6), 131.3 (s, C^8), 131.2 (t, $^3J_{C-F}$ = 9.8, C^4), 119.2 (s, C^7), 118.0 (t, $^2J_{C-F}$ = 21.9, C^1), 111.8 (m, C^3), 27.0 (vt, *N* = 28.0, PCH), 20.6, 19.6 (both s, PCH*C*H$_3$).

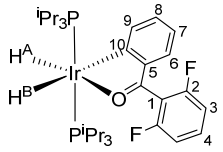

Reaction of Complex 1 with 2-(4-Fluorophenyl)pyridine: Preparation of $IrH_2\{\kappa^2$-*C,N*-$[C_6H_3F$-py$]\}(P^iPr_3)_2$ (6). A colorless solution of **1** (100 mg, 0.193 mmol) in 10 mL of toluene was treated with 2-(4-fluorophenyl)pyridine (34 mg, 0.193 mmol) and heated under reflux. After 16 h, the solvent was removed under vacuum and methanol was added to afford a yellow solid, which was washed with methanol at -78 °C and vacuum-dried. Yield: 120 mg (87%). Anal. Calcd for $C_{29}H_{51}FIrNP_2$: C, 50.71; H, 7.48; N, 2.04. Found: C, 50.56; H, 7.75; N, 2.16. HRMS (electrospray, *m*/*z*): Calcd for $C_{29}H_{50}FIrNP_2$ $[M - H]^+$ 686.3026; found: 686.3014. IR (cm^{-1}): ν(IrH) 2216 (w), 1990 (w). ^1H NMR (300, MHz, C_6D_6, 298 K): δ 9.19 (br d, $^3J_{H\text{-}H}$ = 5.7, 1H, H^6), 8.20 (br d, $^3J_{H\text{-}F}$ = 9.9, 1H, H^{11}), 7.59 (dd, $^3J_{H\text{-}H}$ = 8.6, $^4J_{H\text{-}F}$ = 5.4, 1H, H^8), 7.37 (br d, $^3J_{H\text{-}H}$ = 7.7, 1H, H^3), 6.98 (dd, $^3J_{H\text{-}H}$ = $^3J_{H\text{-}H}$ = 7.7, 1H, H^4), 6.85 (ddd, $^3J_{H\text{-}H}$ = $^3J_{H\text{-}F}$ = 8.6, $^4J_{H\text{-}H}$ = 2.8, 1H, H^9), 6.27 (ddd, $^3J_{H\text{-}H}$ = 7.7, $^3J_{H\text{-}H}$ = 5.7, $^4J_{H\text{-}H}$ = 1.4, 1H, H^5), 1.93 (m, 6H, PCH), 0.99 (dvt, *N* = 13.2, $^3J_{H\text{-}H}$ = 6.8, 18 H, PCHC*H*$_3$), 0.93 (dvt, *N* = 12.9, $^3J_{H\text{-}H}$ = 6.9, 18 H, PCHC*H*$_3$), −12.65 (m, 1H, IrH^B), −20.87 (td, $^2J_{H\text{-}P}$ = 18.6, $^2J_{H\text{-}H}$ = 4.7, 1H, IrH^A). $^{31}P\{^1H\}$ NMR (121.42, MHz, C_6D_6, 298 K): δ 26.2 (s). ^{19}F NMR (282.33, MHz, C_6D_6, 298 K): δ −114.8 (ddd, $^3J_{F\text{-}H}$ = 9.9, $^3J_{F\text{-}H}$ = 8.6, $^4J_{F\text{-}H}$ = 5.4). $^{19}F\{^1H\}$ NMR (282.33, MHz, C_6D_6, 298 K): δ −114.8. $^{13}C\{^1H\}$ NMR (75.42, MHz, C_6D_6): δ 182.3 (td, $^2J_{C\text{-}P}$ = 7.0, $^4J_{C\text{-}F}$ = 3.1, IrC^{12}), 168.8 (s, C_q^2), 164.2 (d, $^1J_{C\text{-}F}$ = 252.7, $C^{10}F$), 157.9 (s, C^6), 144.2 (s, C_q^7), 134.2 (s, C^4), 129.2 (d, $^2J_{C\text{-}F}$ = 12.9, C^{11}), 126.3 (d, $^3J_{C\text{-}F}$ = 8.3, C^8), 120.1 (s, C^5), 118.7 (s, C^3), 107.0 (d, $^2J_{C\text{-}F}$ = 23.6, C^9), 26.8 (vt, *N* = 27.5, PCH), 20.0, 19.7 (both s, PCH*C*H$_3$).

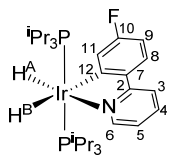

Reaction of Complex 1 with 2-(2,4-Difluorophenyl)pyridine: Formation of 6 and [$IrH_2\{\kappa^2$-*C,N*-($C_6H_2F_2$-py}(P^iPr_3)$_2$] (7). A solution of **1** (100 mg, 0.193 mmol) in 10 mL of toluene was treated with 2-(2,4-difluorophenyl)pyridine (0.030 mL, 0.193 mmol) and heated under reflux. After 4 h, the solvent was removed under vacuum and methanol was added to afford a yellow solid, which was washed with methanol at -78 °C and vacuum-dried. NMR spectra of this solid showed the presence of a mixture of **6** and **7** in a 1:9 molar ratio. Combined yield: 80 mg. X-ray crystals were grown in a concentrated solution of benzene-d_6 at 4 ºC. Complex **7** and **6** co-crystallized in a 9:1 ratio. HRMS (electrospray, *m*/*z*): Calcd for $C_{29}H_{49}F_2IrNP_2$ $[M - H]^+$ 704.2932; found: 704.2914. IR (cm^{-1}): ν(IrH) 2217 (w), 2001 (w). NMR data for **7**: ^{1}H NMR (300, MHz, C_6D_6, 298 K): δ 9.23 (br d, $^3J_{H\text{-}H}$ = 5.6, 1H, H^6 py), 8.36 (m, 1H, H^3 py), 7.99 (br d, $^3J_{H\text{-}F}$ = 8.6, 1H, H^{11}), 7.02 (m, 1H, H^4 py), 6.60 (ddd, $^3J_{H\text{-}F}$ = 13.5, $^3J_{H\text{-}F}$ = 8.6, $^4J_{H\text{-}H}$ = 2.4, 1H, H^9), 6.25 (ddd, $^3J_{H\text{-}H}$ = 7.5, $^3J_{H\text{-}H}$ = 5.6, $^4J_{H\text{-}H}$, 1.4 = 1H, H^5 py), 1.90 (m, 6H, PCH), 0.95 (dvt, *N* = 13.2, $^3J_{H\text{-}H}$ = 6.4, 18 H, PCHC*H*$_3$), 0.91 (dvt, *N* = 12.7, $^3J_{H\text{-}H}$ = 6.0, 18 H, PCHC*H*$_3$), −12.85 (m, 1H, IrH^B), −20.85 (td, $^2J_{H\text{-}P}$ = 18.6, $^2J_{H\text{-}H}$ = 4.7, 1H, IrH^A). $^{31}P\{^1H\}$ NMR (121.42, MHz, C_6D_6, 298 K): δ 26.2 (s). ^{19}F NMR (282.33, MHz, C_6D_6, 298 K): δ −110.9 (m, 1F), −113.0 (m, 1F). $^{19}F\{^1H\}$ NMR (282.33, MHz, C_6D_6, 298 K): δ −110.9 (d, $^4J_{F\text{-}F}$ = 8.6, 1F), −113.0 (d, $^4J_{F\text{-}F}$ = 8.6, 1F). $^{13}C\{^1H\}$ NMR (75.42, MHz, C_6D_6): δ 185.7 (tdd, $^2J_{C\text{-}P}$ = 6.6, $^3J_{C\text{-}F}$ = 2.7, IrC^{12}), 166.3 (d, $^3J_{C\text{-}F}$ = 8.0, C_q^2 py), 163.6 (dd, $^1J_{C\text{-}F}$ = 261.0, $^3J_{C\text{-}F}$ = 11.0, C^8F or $C^{10}F$), 163.4 (dd, $^1J_{C\text{-}F}$ = 256.4, $^3J_{C\text{-}F}$ = 10.5, C^8F or $C^{10}F$), 157.9 (s, C^6 py), 134.8 (s, C^4 py), 131.3 (s, C_q^7), 124.8 (dd, $^2J_{C\text{-}F}$ = 12.3, $^4J_{C\text{-}F}$ = 2.9, C^{11}), 123.1 (d, $^4J_{C\text{-}F}$ = 23.0, C^3 py), 120.5 (s, C^5 py), 95.5 (dd, $^2J_{C\text{-}F}$ = $^2J_{C\text{-}F}$ = 27.6, C^9), 26.7 (vt, *N* = 27.6, PCH), 19.9, 19.6 (both s, PCH*C*H$_3$).

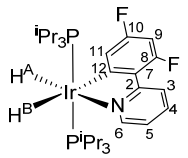

Reaction of Complex 1 with 2,6-bis(2,4-Difluorophenyl)pyridine in Toluene: Formation of [IrH{κ^3-*C,N,C*-($C_6H_2F_2$-py-$C_6H_2F_2$}(P^iPr_3)$_2$] (8). A colorless solution of **1** (100 mg, 0.193 mmol) in 10 mL of toluene was treated with 2,6-bis(2,4-difluorophenyl)pyridine (70.1 mg, 0.193 mmol) and heated under reflux. After 40 h, the solvent was removed under vacuum and methanol was added to afford a yellow solid, which was washed with methanol at -78 °C and vacuum-dried. NMR spectra of this solid showed the presence of a mixture of **8** and **9** in a 65:35 molar ratio. X-ray crystals were grown in a concentrated solution of benzene-d_6 at 4 ºC. Complex **8** and **9** co-crystallized in a 8:2 ratio. HRMS (electrospray, *m*/*z*): Calcd for $C_{35}H_{50}F_4IrNP_2$ $[M + Na]^+$ 838.2882; found: 838.8383. IR (cm^{-1}): *ν*(IrH) 2222 (w). NMR data for **8**: ^{1}H NMR (300, MHz, C_6D_6, 298 K): δ 8.10 (d, $^3J_{H\text{-}H}$ = 8.7, 2H, H^3, H^5), 7.60 (m, 2H, H^{11}), 7.19 (dd, $^3J_{H\text{-}H}$ = $^3J_{H\text{-}H}$ = 8.2, 1H, H^4), 6.57 (ddd, $^3J_{H\text{-}F}$ = 13.1, $^4J_{H\text{-}F}$ = 8.9, $^4J_{H\text{-}H}$ = 2.5, 2H, H^9), 2.01 (m, 6H, PCH), 0.78 (m, 36 H, PCHC*H*$_3$), −15.52 (t, $^2J_{H\text{-}P}$ = 19.8, 1H, IrH). ^{31}P{^{1}H} NMR (121.42, MHz, C_6D_6, 298 K): δ 4.3 (s). ^{19}F NMR (282.33, MHz, C_6D_6, 298 K): δ −111.1 (m, 2F), −111.3 (m, 2F). ^{19}F{^{1}H} NMR (282.33, MHz, C_6D_6, 298 K): δ −111.2 (AB spin system, Δν = 53.6, J_{AB} = 8.5). ^{13}C{^{1}H} NMR (75.42, MHz, C_6D_6): δ 171.5 (m, IrC^{12}), 164.2 (s, C_q^6 or C_q^7), 163.6 (dd, $^1J_{C\text{-}F}$ = 257.1, $^3J_{C\text{-}F}$ = 11.7, C^8F or $C^{10}F$), 163.5 (dd, $^1J_{C\text{-}F}$ = 263.5, $^3J_{C\text{-}F}$ = 11.5, C^8F or $C^{10}F$), 137.0 (s, C^4 py), 134.7 (s, C_q^6 or C_q^7), 122.8 (d, $^2J_{C\text{-}F}$ = 13.4, C^{11}), 117.9 (d, $^4J_{C\text{-}F}$ = 21.4, C^3, C^5 py), 96.8 (dd, $^2J_{C\text{-}F}$ = $^2J_{C\text{-}F}$ = 27.1, C^9), 26.2 (vt, *N* = 27.9, PCH), 18.8 (s, PCH*C*H$_3$).

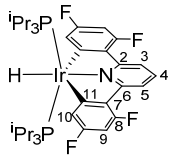

Reaction of Complex 1 with 2,6-Bis(2,4-difluorophenyl) pyridine in Decalin: Formation of [IrH{κ^3-*C,N,C*-($C_6H_2F_2$-py-C_6H_3F}(P^iPr_3)$_2$] (9). A colorless solution of **1** (100 mg, 0.193 mmol) in 10 mL of decalin was treated with 2,6-bis(2,4-difluorophenyl)pyridine (70.1 mg, 0.193 mmol) and heated under reflux. After 4 h, the solvent was removed under vacuum and methanol was added to afford a yellow solid, which was washed with methanol at -78 °C and vacuum-dried. NMR spectra of this solid showed the presence of a mixture of **8** and **9** in a 1:9 molar ratio. X-ray crystals were grown in a concentrated solution of benzene-d_6 at 4 ºC. Complex **8** and **9** co-crystallized in a 3:7 ratio. HRMS (electrospray, *m*/*z*): Calcd for $C_{35}H_{51}F_3IrNP_2$ $[M]^+$ 797.3078; found: 797.3071. IR (cm^{-1}): *ν*(IrH) 2222 (w). NMR data for **9**: ^{1}H NMR (300, MHz, C_6D_6, 298 K): δ 8.12 (dd, $^3J_{H\text{-}H}$ = 7.2, $^4J_{H\text{-}H}$ = 1.5, 1H, H^5 py), 7.80 (m, 1H, H^{17}), 7.65 (m, 1H, H^{11}), 7.43 (dd, $^3J_{H\text{-}H}$ = 8.6, $^4J_{H\text{-}F}$ = 5.8, 1H, H^{14}), 7.19 – 7.10 (2H, H$^{3\text{-}4}$ py), 6.80 (ddd, $^3J_{H\text{-}H}$ = 8.6, $^3J_{H\text{-}F}$ = 8.6, $^4J_{H\text{-}H}$ = 2.6, 1H, H^{15}), 6.59 (ddd, $^3J_{H\text{-}F}$ = 12.2, $^3J_{H\text{-}F}$ = 9.3, $^4J_{H\text{-}H}$ = 2.4, 1H, H^9), 2.03 (m, 6H, PCH), 0.79 (m, 36 H, PCHC*H*$_3$), −15.47 (t, $^2J_{H\text{-}P}$ = 19.8, 1H, IrH). ^{31}P{^{1}H} NMR (121.42, MHz, C_6D_6, 298 K): δ 4.5 (s). ^{19}F NMR (282.33, MHz, C_6D_6, 298 K): δ −111.3 (m, 2F, $C_6H_2F_2$), −112.7 (m, 1F, C_6H_3F). ^{19}F{^{1}H} NMR (282.33, MHz, C_6D_6, 298 K): δ −111.3 (AB spin system, Δν = 14.7, J_{AB} = 8.4, 2F, $C_6H_2F_2$), −112.7 (s, 1F, C_6H_3F). ^{13}C{^{1}H} NMR (75.42, MHz, C_6D_6): δ 172.5 (m, IrC^{12}), 168.3 (td, $^3J_{C\text{-}P}$ = 9.0, $^4J_{C\text{-}F}$ = 2.2, IrC^{18}), 166.5 (s, C$_q^2$ py), 164.3 (s, C$_q^6$ or C$_q^7$), 164.1 (d, $^1J_{C\text{-}F}$ = 252.6, C^{16}F), 163.6 (dd, $^1J_{C\text{-}F}$ = 256.5, $^3J_{C\text{-}F}$ = 11.2, C^{8}F or C^{10}F), 162.5 (dd, $^1J_{C\text{-}F}$ = 258.9, $^3J_{C\text{-}F}$ = 11.8, C^{8}F or C^{10}F), 147.3 (s, C$_q^{13}$), 136.4 (s, CH^3 or CH^4 py), 134.7 (s, C$_q^6$ or C$_q^7$), 127.1 (d, $^2J_{C\text{-}F}$ = 13.9, C^{17}), 125.9 (d, $^3J_{C\text{-}F}$ = 8.4, C^{14}), 122.8 (dd, $^2J_{C\text{-}F}$ = 12.8, $^4J_{C\text{-}F}$ = 2.8, C^{11}), 117.4 (d, ^{4}J$_{C\text{-}F}$ =

20.3, C^5 py), 113.2 (s, CH^3 or CH^4 py), 108.2 (d, $^2J_{C\text{-}F}$ = 23.1, C^{15}), 96.6 (dd, $^2J_{C\text{-}F}$ = $^2J_{C\text{-}F}$ = 26.9, C^9), 26.2 (vt, *N* = 27.8, PCH), 18.8, 18.8 (both s, PCH*C*H$_3$).

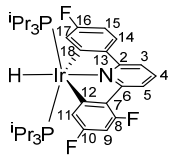

General Procedure for the Reactions with IrD$_5$(PiPr$_3$)$_2$ (1*d*$_5$). The reactions were carried under the same conditions as the reactions with **1**, starting from **1*d*$_5$** (50 mg, 0.095 mmol), the corresponding ketone or pyridine (0.095 mmol), and toluene-d_8 (1 mL). The deuterium incorporation was measured in the ^{1}H NMR spectrum of the product in C_6D_6.

ASSOCIATED CONTENT

Supporting Information. The Supporting Information is available free of charge on the ACS Publications website.

General information for the experimental section, NMR spectra, and structural analysis (PDF)

Accession Codes

CCDC 2360620-2360624 contain the supplementary crystallographic data. They can be obtained free of charge via www.ccdc.cam.ac.uk/data_request/cif, or by emailing data_ request@ccdc.cam.ac.uk, or by contacting The Cambridge Crystallographic Data Centre, 12 Union Road, Cambridge CB2 1EZ, UK; fax: +44 1223 336033

AUTHOR INFORMATION

Corresponding Author

* E-mail: maester@unizar.es

Author Contributions

The manuscript was written through contributions of all authors. All authors have given approval to the final version of the manuscript.

Notes

The authors declare no competing financial interests.

ACKNOWLEDGMENT

Financial support from MICIN/AEI/10.13039/501100011033 (PID2020-115286GB-I00 and RED2022-134287-T), Gobierno de Aragón (E06_23R), FEDER, and the European Social Fund is acknowledged.

REFERENCES

(1) (a) Hartwig, J. F. Evolution of C−H Bond Functionalization from Methane to Methodology. *J. Am. Chem. Soc.* **2016**, *138*, 2−24. (b) Gunsalus, N. J.; Koppaka, A.; Park, S. H.; Bischof, S. M.; Hashiguchi, B. G.; Periana, R. A. Homogeneous Functionalization of Methane. *Chem. Rev.* **2017**, *117*, 8521−8573. (c) Dalton, T.; Faber, T.; Glorius, F. C–H Activation: Toward Sustainability and Applications. *ACS Cent. Sci.*, **2021**, *7*, 245−261. (d) Jana, R.; Begam, H. M.; Dinda, E. The emergence of the C–H functionalization strategy in medicinal chemistry and drug discovery. *Chem. Commun.* **2021**, *57*, 10842−10866.

(2) (a) Jones, W. D.; Feher, F. J. Comparative reactivities of hydrocarbon carbon-hydrogen bonds with a transition-metal complex. *Acc. Chem. Res.* **1989**, *22*, 91−100. (b) Shilov, A. E.; Shul'pin, G. B. Activation of C−H Bonds by Metal Complexes. *Chem. Rev.* **1997**, *97*, 2879−2932. (c) Balcells, D.; Clot, E.; Eisenstein, O. C−H Bond Activation in Transition Metal Species from a Computational Perspective. *Chem. Rev.* **2010**, *110*, 749−823. (d) Pabst, T. P.; Chirik, P. J. A

Tutorial on Selectivity Determination in C(sp^2)–H Oxidative Addition of Arenes by Transition Metal Complexes. *Organometallics* **2021**, *40*, 813−831.

(3) (a) Mkhalid, I. A. I.; Barnard, J. H.; Marder, T. B.; Murphy, J. M.; Hartwig, J. F. C−H Activation for the Construction of C−B bonds. *Chem. Rev.* **2010**, *110*, 890−931. (b) Davies, H. M.; Morton, D. Recent advances in C–H functionalization. *J. Org. Chem.* **2016**, *81*, 343−350. (c) Hartwig, J. F.; Larsen, M. A. Undirected, Homogeneous C–H Bond Functionalization: Challenges and Opportunities. *ACS Cent. Sci.* **2016**, *2*, 281−292.

(4) (a) Esteruelas, M. A.; López, A. M. C−C Coupling and C−H Bond Activation Reactions of Cyclopentadienyl−Osmium Compounds: The Rich and Varied Chemistry of Os(η^5-C_5H_5)Cl(P^iPr_3)$_2$ and Its Major Derivatives. *Organometallics* **2005**, *24*, 3584−3613. (b) Werner, H. Carbene–Transition Metal Complexes Formed by Double C–H Bond Activation. *Angew. Chem., Int. Ed.* **2010**, *49*, 4714−4728.

(5) (a) He, J.; Wasa, M.; Chan, K. S. L.; Shao, Q.; Yu, J.-Q. Palladium-Catalyzed Transformations of Alkyl C–H Bonds. *Chem. Rev.* **2017**, *117*, 8754−8786. (b) Wei, Y.; Hu, P.; Zhang, M.; Su, W. Metal-Catalyzed Decarboxylative C–H Functionalization. *Chem. Rev.* **2017**, *117*, 8864−8907. (c) Newton, C. G.; Wang, S.-G.; Oliveira, C. C.; Cramer, N. Catalytic Enantioselective Transformations Involving C–H Bond Cleavage by Transition-Metal Complexes. *Chem. Rev.* **2017**, *117*, 8908−8976. (d) Hummel, J. R.; Boerth, J. A.; Ellman, J. A. Transition-Metal-Catalyzed C–H Bond Addition to Carbonyls, Imines, and Related Polarized π Bonds. *Chem. Rev.* **2017**, *117*, 9163−9227. (e) Park, Y.; Kim, Y.; Chang, S. Transition Metal-Catalyzed C–H Amination: Scope, Mechanism, and Applications. *Chem. Rev.* **2017**, *117*, 9247−9301. (f) Dong,

Z.; Ren, Z.; Thompson, S. J.; Xu, Y.; Dong, G. Transition-Metal-Catalyzed C–H Alkylation Using Alkenes. *Chem. Rev.* **2017**, *117*, 9333−9403.

(6) (a) Chi, Y.; Chou. P.-T. Transition-metal phosphors with cyclometalating ligands: fundamentals and applications. *Chem. Soc. Rev*. **2010**, *39*, 638−655. (b) Caporale, C.; Massi, M. Cyclometalated iridium(III) complexes for life science. *Coord. Chem. Rev*. **2018**, *363*, 71−91. (c) Yoon, S.; Teets, T. S. Red to near-infrared phosphorescent Ir(III) complexes with electron-rich chelating ligands. *Chem. Commun*. **2021**, *57*, 1975−1988. (d) Buil, M. L.; Esteruelas, M. A.; López, A. M. Recent Advances in Synthesis of Molecular Heteroleptic Osmium and Iridium Phosphorescent Emitters. *Eur. J. Inorg. Chem*. **2021**, 4731–4761.

(7) (a) Banks, R. E.; Smart, B. E.; Tatlow, J. C. Eds. Organofluorine Chemistry: Principles and Commercial Applications; Springer: Media New York, 1994. (b) Kirsch, P. Modern Fluoroorganic Chemistry: Synthesis, Reactivity, and Applications; Wiley-VCH: Weinheim, 2004.

(8) (a) Müller, K.; Faeh, C.; Diederich, F. Fluorine in Pharmaceuticals: Looking Beyond Intuition. *Science* **2007**, *317*, 1881–1886. (b) Purser, S.; Moore, P. R.; Swallow S.; Gouverneur, V. Fluorine in medicinal chemistry. *Chem. Soc. Rev*. **2008**, *37*, 320-330. (c) Hagmann, W. K. The Many Roles for Fluorine in Medicinal Chemistry. *J. Med. Chem*. **2008**, *51*, 4359–4369. (d) O'Hagan, D. Fluorine in health care: Organofluorine containing blockbuster drugs. *J. Fluor. Chem*. **2010**, *131*, 1071–1081. (e) Inoue, M.; Sumii, Y.; Shibata, N. Contribution of Organofluorine Compounds to Pharmaceuticals. *ACS Omega* **2020**, *5*, 10633–0640.

(9) (a) Jeschke, P. The Unique Role of Fluorine in the Design of Active Ingredients for Modern Crop Protection. *ChemBioChem* **2004**, *5*, 570–589. (b) Jeschke, P. The unique role of halogen substituents in the design of modern agrochemicals. *Pest Manag. Sci*. **2010**, *66*, 10–27. (c)

Fujiwara, T.; O'Hagan, D. Successful fluorine-containing herbicide agrochemicals. *J. Fluor. Chem*. **2014**, *167*, 16–29. (d) Ogawa, Y.; Tokunaga, E.; Kobayashi, O.; Hirai, K.; Shibata, N. Current Contributions of Organofluorine Compounds to the Agrochemical Industry. *iScience* **2020**, *23*, 101467.

(10) Wang, J.; Sánchez-Roselló, M.; Aceña, J. L.; del Pozo, C.; Sorochinsky, A. E.; Fustero, S.; Soloshonok, V. A.; Liu, H. Fluorine in Pharmaceutical Industry: Fluorine-Containing Drugs Introduced to the Market in the Last Decade (2001−2011). *Chem. Rev*. **2014**, *114*, 2432−2506.

(11) (a) Sun, A. D.; Love, J. A. Cross coupling reactions of polyfluoroarenes *via* C–F activation. *Dalton Trans*. **2010**, *39*, 10362−10374. (b) Ahrens, T.; Kohlmann, J.; Ahrens, M.; Braun, T. Functionalization of Fluorinated Molecules by Transition-Metal-Mediated C−F Bond Activation To Access Fluorinated Building Blocks. *Chem. Rev*. **2015**, *115*, 931−972. (c) Xu, W.; Zhang, Q.; Shao, Q.; Xia, C.; Wu, M. Photocatalytic C F Bond Activation of Fluoroarenes, gem-Difluoroalkenes and Trifluoromethylarenes. *Asian J. Org. Chem*. **2021**, *10*, 2454−2472. (d) Wang, K.; Kong, W. Synthesis of Fluorinated Compounds by Nickel-Catalyzed Defluorinative Cross-Coupling Reaction. *ACS Catal*. **2023**, *13*, 12238−12268. (e) Hooker, L. V.; Bandar, J. S. Synthetic Advantages of Defluorinative C−F Bond Functionalization. *Angew. Chem. Int. Ed*. **2023**, *62*, e202308880. (f) Budiman, Y. P.; Perutz, R. N.; Steel, P. G.; Radius, U.; Marder, T. B. Applications of Transition Metal-Catalyzed *ortho*-Fluorine-Directed C−H Functionalization of (Poly)fluoroarenes in C−F Bond Activation at Fluorocarbons. Organic Synthesis. *Chem. Rev*. **2024**, *124*, 4822−4862.

(12) Luo, Y.-R. *Comprehensive Handbook of Chemical Bond Energies*; CRC Press: Boca Raton, 2007.

(13) Eisenstein, O.; Milani, J.; Perutz, R. N. Selectivity of C−H Activation and Competition between C−H and C−F Bond Activation at Fluorocarbons. *Chem. Rev*. **2017**, *117*, 8710−8753.

(14) Selmeczy, A. D.; Jones, W. D.; Partridge, M. G.; Perutz, R. N. Selectivity in the Activation of Fluorinated Aromatic Hydrocarbons by [(C_5H_5)Rh(PMe_3)] and [(C_5Me_5)Rh(PMe_3)]. *Organometallics* **1994**, *13*, 522−532.

(15) Esteruelas, M. A.; Martínez, A.; Oliván, M.; Oñate, E. Kinetic Analysis and Sequencing of Si−H and C−H Bond Activation Reactions: Direct Silylation of Arenes Catalyzed by an Iridium-Polyhydride. *J. Am. Chem. Soc*. **2020**, *142*, 19119−19131.

(16) For Fe, see: (a) Xu, X.; Sun, H.; Shi, Y.; Jia, J.; Li, X. Imine-assisted C–F bond activation by electron-rich iron complexes supported by trimethylphosphine. *Dalton Trans*. **2011**, *40*, 7866−7872. (b) Wang, L.; Sun, H.; Li, X. Synthesis of Iron Hydrides by Selective C–F/C–H Bond Activation in Fluoroarylimines and Their Applications in Catalytic Reduction Reactions. *Eur. J. Inorg. Chem*. **2015**, 2732−2743.

(17) For Ru, see: (a) A. Diggle, R.; Kennedy, A. A.; Macgregor, S. A.; Whittlesey, M. K. Computational Studies of Intramolecular Carbon-Heteroatom Bond Activation of N-Aryl Heterocyclic Carbene Ligands. *Organometallics* **2008**, *27*, 938−944. (b) Alós, J.; Esteruelas, M. A.; Oliván, M.; E.; Oñate, Puylaert, P. C−H Bond Activation Reactions in Ketones and Aldehydes Promoted by POP-Pincer Osmium and Ruthenium Complexes. *Organometallics* **2015**, *34*, 4908−4921.

(18) For Os, see ref 17b and: (a) Barrio, P.; Castarlenas, R.; Esteruelas, M. A.; Lledós, A.; Maseras, F.; Oñate, E.; Tomàs, J. Reactions of a Hexahydride-Osmium Complex with Aromatic Ketones: C-H Activation versus C-F Activation. *Organometallics* **2001**, *20*, 442−452. (b)

Esteruelas, M. A.; Lledós, A.; Oliván, M.; Oñate, E.; Tajada, M. A.; Ujaque, G. *Ortho*-CH Activation of Aromatic Ketones, Partially Fluorinated Aromatic Ketones, and Aromatic Imines by a Trihydride-Stannyl-Osmium(IV) Complex. *Organometallics* **2003**, *22*, 3753−3765.

(19) For Co, see: (a) Camadanli, S.; Beck, R.; Flörkec, U.; Klein, H.-F. First regioselective cyclometalation reactions of cobalt in arylketones: C–H *versus* C–F activation. *Dalton Trans*. **2008**, 5701−5704. (b) T.; Zheng, Sun, H.; Ding, J.; Zhang, Y.; Li, X. Effect of anchoring group and valent of cobalt center on the competitive cleavage of C−F or C−H bond activation. *J. Organomet. Chem*. **2010**, *695*, 1873−1877. (c) Li, J.; Zhang, D.; Sun H.; Li, X. Computational rationalization of the selective C–H and C–F activations of fluoroaromatic imines and ketones by cobalt complexes. *Org. Biomol. Chem*. **2014**, *12*, 1897−1907.

(20) For Rh, see: (a) Ballhorn, M.; Partridge, M. G.; Perutz, R. N.; Whittlesey, M. K. Photochemical intermolecular C-H and C-F insertion of rhodium into pentafluoroanisole to generate a metallacycle; conversion to a cyclic carbene complex. *Chem. Commun*. **1996**, 961−962. (b) Li, L.; Brennessel, W. W.; Jones, W. D. C-H activation of phenyl imines and 2-phenylpyridines with $[Cp^*MCl_2]_2$ (M = Ir, Rh): Regioselectivity, kinetics, and mechanism. *Organometallics* **2009**, *28*, 3492−3500. (c) Procacci, B.; Blagg, R. J.; Perutz, R. N.; Rendón, N.; Whitwood, A. C. Photochemical Reactions of Fluorinated Pyridines at Half-Sandwich Rhodium Complexes: Competing Pathways of Reaction. *Organometallics* **2014**, *33*, 45−52.

(21) For Ir, see: (a) Kundu, S.; Choi, J., Wang, D. Y.; Choliy, Y.; Emge, T. J.; Krogh-Jespersen, K. Cleavage of Ether, Ester, and Tosylate $C(sp^3)$−O Bonds by an Iridium Complex, Initiated by Oxidative Addition of C−H Bonds Experimental and Computational Studies. *J. Am. Chem. Soc*. **2013**, *135*, 5127−5143. (b) Porras, J. A.; Mills, I. N.; Transue, W. J.; Bernhard, S. Highly

Fluorinated Ir(III)−2,2':6',"-Terpyridine−Phenylpyridine−X Complexes via Selective C−F Activation: Robust Photocatalysts for Solar Fuel Generation and Photoredox Catalysis. *J. Am. Chem. Soc*. **2016**, *138*, 9460−9472. (c) Laviska, D. A.; Zhou, T.; Kumar, A.; Emge, T. J.; Krogh-Jespersen, K.; Goldman, A. S. Single and Double C-H Activation of Biphenyl or Phenanthrene. An Example of C-H Addition to Ir(III) More Facile than Addition to Ir(I). *Organometallics* **2016**, *35*, 1613−1623. (d) Wilklow-Marnell, M.; Brennessel, W. W.; Jones, W. D. C(sp^2)−F Oxidative Addition of Fluorinated Aryl Ketones by ^{iPr}PCPIr. *Organometallics* **2017**, *36*, 3125−3134. (e) A.; Matsunami, Y.; Kayaki, S.; Kuwata, Ikariya, T. Nucleophilic Aromatic Substitution in Hydrodefluorination Exemplified by Hydridoiridium(III) Complexes with Fluorinated Phenylsulfonyl-1,2-diphenylethylenediamine Ligands. *Organometallics* **2018**, *37*, 1958−1969.

(22) For Ni, see: Mangin, L. P.; Zargarian, D. C–H nickellation of phenol-derived phosphinites: regioselectivity and structures of cyclonickellated complexes. *Dalton Trans*. **2017**, *46*, 16159–16170.

(23) For Pd, see: Milani, J.; Pridmore, N. E.; Whitwood, A. C.; Fairlamb, I. J. S.; Perutz, R. N. The Role of Fluorine Substituents in the Regioselectivity of Intramolecular C−H Bond Functionalization of Benzylamines at Palladium(II). *Organometallics* **2015**, *34*, 4376–4386.

(24) For Pt, see: (a) Crespo, M. Fluorine in Cyclometalated Platinum Compounds. *Organometallics* **2012**, *31*, 1216–1234. (b) T.; Wang, L.; Keyes, Patrick, B. O.; Love, J. A. Exploration of the Mechanism of Platinum(II)-Catalyzed C−F Activation: Characterization and Reactivity of Platinum(IV) Fluoroaryl Complexes Relevant to Catalysis. *Organometallics* **2012**, *31*, 1397–1407.

(25) Esteruelas, M. A.; López, A. M.; Oliván, M. Polyhydrides of Platinum Group Metals: Nonclassical Interactions and σ-Bond Activation Reactions. *Chem. Rev*. **2016**, *116*, 8770−8847.

(26) Babón, J. C.; Esteruelas, M. A.; López, A. M. Homogeneous catalysis with polyhydride complexes. *Chem. Soc. Rev*. **2022**, *51*, 9717–9758.

(27) (a) Esteruelas, M. A.; López, A. M.; Oñate, E.; San-Torcuato, A.; Tsai, J.-Y.; Xia, C. Formation of Dinuclear Iridium Complexes by NHC-Supported C−H Bond Activation. *Organometallics* **2017**, *36*, 699−707. (b) Esteruelas, M. A.; Oñate, E.; Palacios, A. U. Selective Synthesis and Photophysical Properties of Phosphorescent Heteroleptic Iridium(III) Complexes with Two Different Bidentate Groups and Two Different Monodentate Ligands. *Organometallics* **2017**, *36*, 1743−1755. (c) Castro-Rodrigo, R.; Esteruelas, M. A.; Gómez-Bautista, D.; Lezáun, V.; López, A. M.; Oliván, M.; Oñate, E. Influence of the Bite Angle of Dianionic C,N,C-Pincer Ligands on the Chemical and Photophysical Properties of Iridium(III) an Osmium(IV) Hydride Complexes. *Organometallics* **2019**, *38*, 3707−3718. (d) Cancela, L.; Esteruelas, M. A.; López, A. M.; Oliván, M.; Oñate, E.; San-Torcuato, A.; Vélez, A. Osmium- and Iridium-Promoted C−H Bond Activation of 2,2′-Bipyridines and Related Heterocycles: Kinetic and Thermodynamic Preferences. *Organometallics* **2020**, *39*, 2102−2115. (e) Buil, M. L.; Esteruelas, M. A.; Izquierdo, S.; Nicasio, A. I.; Oñate, E. N−H and C−H Bond Activations of an Isoindoline Promoted by Iridium- and Osmium-Polyhydride Complexes: A Noninnocent Bridge Ligand for Acceptorless and Base-Free Dehydrogenation of Secondary Alcohols. *Organometallics* **2020**, *39*, 2719−2731. (f) Cancela, L.; Esteruelas, M. A.; Galbán, J.; Oliván, M.; Oñate, E.; Vélez, A.; Vidal, J. C. Electronic Communication in Binuclear Osmium- and Iridium-Polyhydrides. *Inorg. Chem*. **2021**, *60*, 2783−2796. (g) Babón, J. C.; Boudreault, P.-L. T.; Esteruelas, M. A.; Gaona, M. A.; Izquierdo, S.; Oliván, M.; Oñate, E.; Tsai, J.-Y.; Vélez, A. Two Synthetic Tools to Deepen the Understanding

of the Influence of Stereochemistry on the Properties of Iridium(III) Heteroleptic Emitters. *Inorg. Chem*. **2023**, *62*, 19821−19837. (h) Benítez, M.; Buil, M. L.; Esteruelas, M. A.; López, A. M.; Martín-Escura, C.; Oñate, E. C−H, N−H, and O−H Bond Activations to Prepare Phosphorescent Hydride-Iridium(III)-Phosphine Emitters with Photocatalytic Achievement in C−C Coupling Reactions. *Inorg. Chem.* **2024**, 63, 6346−6361.

(28) Werner, H.; Schulz, M.; Esteruelas, M. A.; Oro, L. A. $IrCl_2H(P^iPr_3)_2$ as catalyst precursor for the reduction of unsaturated substrates. *J. Organomet. Chem*. **1993**, *445*, 261−265.

(29) (a) Zhang, X.; Kanzelberger, M.; Emge, T. J.; Goldman, A. S. Selective Addition to Iridium of Aryl C-H Bonds Ortho to Coordinating Groups. Not Chelation-Assisted. *J. Am. Chem. Soc*. **2004**, *126*, 13192−13193. (b) Ortiz-Hernández, M.; Salazar-Pereda, V.; Mendoza-Espinosa, D.; Gomez-Bonilla, M. A.; Cristobal, C.; Ortega-Alfaro, M. C.; Suárez, A.; Sandoval-Chavez, C. I. CH bond activation in aromatic ketones mediated by iridium-tris(pyrazolyl)borate complexes. *Dalton Trans*. **2023**, *52*, 18315–18322.

(30) (a) Morales-Morales, D., Ed.; Pincer Compounds: Chemistry and Applications, 1st ed.; Elsevier: Amsterdam, 2018. (b) Martin, M.; Sola, E. Recent advances in the chemistry of group 9-Pincer organometallics. In *Adv. Organomet. Chem*. **2020**, *73*, 79−193.

(31) Eguillor, B.; Esteruelas, M. A.; Lezáun, V.; Oliván, M.; Oñate, E. Elongated Dihydrogen versus Compressed Dihydride in Osmium Complexes. *Chem. Eur. J.* **2017**, *23*, 1526–1530.

TOC Graphic